ROAD SURFACE MODELLING AND CHARACTERIZATION FROM TERRESTRIAL LiDAR DATA

A. Di Benedetto[1], M. Fiani[1], L. Petti[1], E. Repetto[2]

[1] Department of Civil Engineering, University of Salerno, Fisciano (SA), Italy – (adibenedetto, m.fiani, petti) @unisa.it
[2] Sipal SpA - repetto.elena@sipal.it

KEY WORDS: LiDAR, MLS, Infrastructure, Monitoring, Distress, Roughness, Rut Depth

ABSTRACT:

The general purpose of the paper is the study of surveying and data processing methodologies that are efficient to obtain more detailed metric data on road infrastructures than can be derived from classical surveying techniques. The inspection and monitoring of the condition of an infrastructure are two essential steps to increase the users' safety and to properly manage the available resources and are a preparatory step to the subsequent steps of deciding on the interventions to be put in place. Analysis of the state of degradation, if conducted with traditional methodologies, can be risky and sometimes inefficient. The Mobile Laser Scanner (MLS) technique, based on LiDAR (Light Detection and Ranging) technology, is also widely used today as an alternative to traditional techniques since it allows obtaining dense and accurate point clouds of the road surface. The purpose of our work is to provide a workflow for the processing of MLS data aimed at producing some useful indicators to describe the functional and structural characteristics of the pavement, with the goal of optimizing the decision-making processes of the Managing Authority. Specifically, the data flow was studied, and several processing algorithms were implemented to identify and quantify surface defects and road roughness. The result of the entire process is the creation of an Atlas in QGIS to create graphical tables related to each individual cross profile and that can be used to identify all those sections that need emergency actions and therefore characterized by a high priority of intervention.

1. INTRODUCTION

The life cycle of the pavement of a civil road infrastructure is made up of several steps: design, construction (which includes both new construction and conservation, maintenance, and rehabilitation), use and finally end of life. According to Life Cycle Assessment (LCA), monitoring of road pavements is crucial as they are subject to degradation (Harvey et al., 2014). Users' safety can be guaranteed only if continuous monitoring operations are performed over time. Thus, the use of expeditious and innovative systems for monitoring deterioration allows for better allocation of resources and thus optimization of management operations in time. The conditions of the road pavement are defined by specific or global performance indices, which are used to assess the conditions of regularity by means of numerical values and evaluation scales (Farias et al., 2009). Roughness is the parameter that most affects the quality of driving and thereby the safety of users; several studies have suggested that the accident rate increases with increasing unevenness of the road surface. Localized distresses are especially worth of interest, as they significantly reduce the safety of users. The huge potential has driven several researchers to establish guidelines on the proper use of the data for infrastructure monitoring (Guan et al., 2016). The most recent systems consist of one or more passive and/or active sensors capable of acquiring dense and accurate data (Ragnoli et al., 2018). The detection of pavement distress (ASTM D6433-18, 2018) in recent years is relying on digital image analysis (Salini et al., 2017; Shen, 2016) and LiDAR (Light Detection and Ranging) data, as traditional techniques, based on manual inspections, are both dangerous to safety and, in most cases, ineffective (De Blasiis et al., 2019a; De Blasiis et al., 2019b; Kumar et al., 2014). LiDAR data produce results that are undoubtedly more accurate than those acquired with traditional techniques (Křemen et al., 2014). Moreover, LiDAR technology has become consolidated over the years, resulting in efficiency, speed, and productivity (Chin, 2012; Glennie, 2009; Yen et al., 2011). The Laser Scanning (LS) technique allows accurate profiles to be acquired and allows the entire road pavement to be analyzed and not individual longitudinal profiles as traditional analyses often do. Several different researchers have used the LS technique to calculate some traditional regularity indicators. Alhasan et al. (2017) uses a dynamic index of pavement regularity on LS data. Chin (2012) studies a methodology for processing LS data so that traditional regularity indices measured in situ can be compared with those derived from LS data. In addition, roughness standard measurements performed using multi-laser profilometers coupled with high precision level have a 99% correlation rate with the data acquired from static LS (Chang et al., 2006). TLS has also been used for the evaluation of faulting on rigid concrete slabs in airport pavements (Barbarella et al., 2018) and for the analysis of the geometry of flexible pavements (Barbarella et al., 2017). MLS technology is currently one of the promising issues in the fields of remote sensing. The assessment of the condition of the road pavement made on MLS data is one of the main objectives of researchers and road Managing Authority, given the high speed data acquisition and the efficiency of the technique (Che et al., 2019; De Blasiis et al., 2020). Mobile Laser Scanners (MLSs), which integrate Laser Scanners (LSs) with inertial platforms and Global Navigation Satellite Systems (GNSS) receivers, enable the fast acquisition of millions of points per second on moving platforms (Gandolfi et al., 2008; Guan et al., 2016). Since the MLS is a multi-sensor system and each sensor is characterized by an error that contributes to the overall accuracy of the survey (Barber et al., 2008; Glennie, 2007), it is also important to analyze them individually in order to estimate the accuracy of overall data (Toschi et al., 2015). The performance of laser sensors has improved greatly over the years and is now possible to acquire point clouds from MLS with greater accuracy. Several researchers have proved the possibility of measuring the height of the scanned points with an accuracy of a few millimeters in the range of distances involved in surveying the road surface (Fryskowska and Wróblewski, 2018). Points clouds acquired by MLS allow digitizing not only the road pavement but also the other elements around it. There are a few studies on the use of MLS for road surveys (Guan et al., 2016), focused on the identification of the paved surface and roadsides, the extraction of road markings and other artifacts such as light poles. Most studies are based on calculating the deviation of points belonging to the road surface from an interpolated plane (roughness) (Kumar et al., 2015). Kumar and Angelats (2017) suggest an automated methodology for the detection of surface defects using morphological operators, multi-Otsu threshold and 3D binary morphological filters applied to a grey-scale intensity surface. MLS

data are also used to classify different types of pavements (asphalt or stone), using K-means algorithms (Díaz-Vilariño et al., 2016). Van der Horst et al. (2019) use k-means clustering to train the Random Forest algorithm to classify different types of distress (craquel, rafeling, longitudinal and transverse cracks, potholes). De Blasiis et al. (2020) present a study on segmentation and classification of some localized distress; they also use as the main parameter the deviation of points belonging to the road pavement with respect to a local interpolated plane. Not so many studies have been published to detect road surface defects from MLS data. Most recent papers point out that data acquired with MLS are currently still being studied in depth, in addition to an increasing interest in these technologies by managing agencies. Mustafa Zeybek and Serkan Biçici (2023) present an interesting pipeline on filtering point clouds acquired by MLS and for computing road geometric attributes such as centerline, profile, cross-section, and cross slope. Chi Liu et al. (2023) reports a detailed review on monitoring infrastructure, specifically tunnels. At the design phase, it is a prerequisite to estimate the minimum resolution/density of the point cloud to be ensured, as the resolution is a function of the MLS acquisition rate and the type of distress to be analyzed. An MLS measurement with no proper design could produce unsuitable data that may not be usable for further analysis. Barbarella et al. (2022) report on a study for determining the ideal resolution of the MLS point cloud as a function of the distress to be analyzed. The authors also present a specific model of the pavement having a curved abscissa with the aim of optimizing the calculation of some indicators of regularity as well as computational effort. Filtering and pre-processing of data are key steps in the process and several researchers are studying and developing algorithms in this respect. Hence, much processing currently is either semiautomatic or manual, depending on the application. Few completely automated procedures exist, and those that do often are found in specialized software packages. Automated ground surface extraction software packages generally work well, however, few of them are optimized for road surface. Some methodologies proposed are based on the identification of the edges of the road surface. Mc Elhinney et al. (2010) extract road shoulders by analyzing the cross sections. Ibrahim and Lichti (2012) describe a method in five steps to detect the curb: organizing the 3D point cloud, nearest neighbor search, 3D density-based segmentation to segment the ground, morphological analysis to refine out the ground segment, derivative of Gaussian filtering to detect the curb. Topology and smoothness of road and the local shape features of point clouds are used by Yang et al. (2013). Kumar et al. (2013) develops a methodology for extracting road curbs by combining elevation values with radiometric data. Guan et al. (2014) implement a methodology for extracting curbs based on geometric analysis of cross sections orthogonal to the MLS trajectory again. Balado et al. (2018) introduced a method based on the use of a combination of geometrical and topological features to classify some elements of street such as, for example, road paving, sidewalks, treads, risers, and curbs. As it may be noted, in the last decade the issue of curbs extraction has received the attention of many researchers, as related in the systematic literature review made by M. Romero et al. (2021).

Other methods are designed for applications where the edges of the road surface are not easily identifiable. Among them, Yoon and Crane (2009) identified the paved surface on the single profiles being extracted by analyzing slopes and standard deviations of elevation values. Yadav et al. (2017) have proposed a method, designed for complex areas, whereby elements and objects that are on the road surface and do not belong there are removed first, then topology and spatial density are analyzed, together with the intensity values to extract the paved surface, and finally the roadside polylines are extracted and geometrically corrected. From the foregoing, it is emerging that the methodologies for the monitoring of surface defects, including those for filtering and extracting the points belonging to the road pavement are many and differ depending on the type of road, the resolution of the data, and the use to be made of it. As a result, it is tricky to identify a precise processing pipeline from filtering to pavement modeling and defects identification.

The goal of our work is to implement a process to analyze the surface deformations of road pavement using MLS data. The proposed methodology is based on the curved abscissa DEM studied by Barbarella et al. (2022) yet optimized to reconstruct the surface even in the presence of shadows and occlusions (vehicles, barriers, etc.). The pavement model will be used in automated processes so as to analyze the deformational state continuously and calculate some state indicators that are required to describe the functional and structural characteristics of the pavement in order to optimize the decision-making processes of the Managing Authority. The optimization of scheduling is aimed at finding the strategies that can maximize the benefits with the same available budget; the MLS technique allows a fast, at operating speed, safe and economical survey of the road pavement and its boundary elements, which is ideal for drawing up an extraordinary program of first intervention quickly and at a very reduced cost.

2. DATA SET

Data were acquired with the Leica Pegasus TRK500 Neo MLS in collaboration with C.U.G.RI. (Inter-University Research Center for the Prediction and Prevention of Major Hazards), Leica Geosystems for the survey and the Consorzio Stabile SIS S.c.p.a. for logistical support, on a 4.8 km long section of the A3 highway (Figure 1a) (Campania Region, Italy), specifically on the southern carriageway from Vietri sul Mare toll gate (km 46+800) to Salerno North (km 51+600) (Figure 1a, b). The travel speed along the road section was about 20 km/h. The output is a point cloud, georeferenced in UTM/RDN2008, with maximum density of about 5,000 points/m^2 along the MLS trajectory, a minimum density of 1,000 points/m^2 at the distance of about 5 m from the MLS center (Figure 1c). The average distance between two scan lines is 2.3 cm.

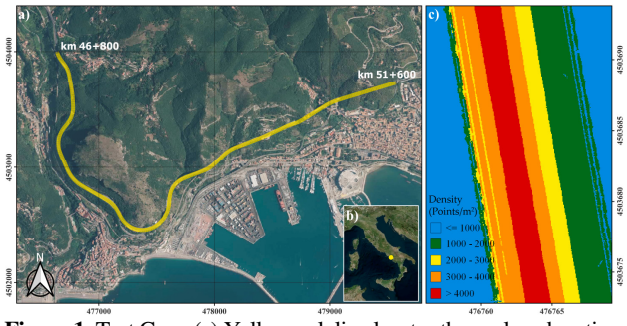

Figure 1. Test Case, (a) Yellow polyline locates the analyzed section, on Google Earth map; (b) Italy map, yellow dot pinpoints the test area; (c) Density map regarding an excerpt of the entire South roadway (Points/m^2).

3. METHODS

Data processing involves three main steps:

1. The first step focuses on editing the point cloud. To identify surface defects and road roughness, the acquired point clouds are not directly usable, but must first be filtered to remove points that do not belong to the road pavement surface (vegetation, cars, pedestrians, etc.).
2. The second step involves the implementation of a specific algorithm able of generating a curved abscissa grid DEM (DEMc). The abscissa axis of the grid has to follow the axis of the horizontal road markings. Since the road belt usually includes straight and curved sections, a grid DEM with North-South direction would not be suitable for modeling its surface.
3. The last step consists of both evaluating the roughness of the road (via regularity indices) and calculating the main geometric parameters of each single profile extracted from the DEMc (longitudinal and cross-sectional).

Figure 2 shows the workflow of the procedure. Each output is organized to produce an Atlas in a semi-automatic way in QGIS environment. In particular, the output consists in shapefiles for numerical data and in .svg images for plots. All processes have been implemented in MATLAB environment.

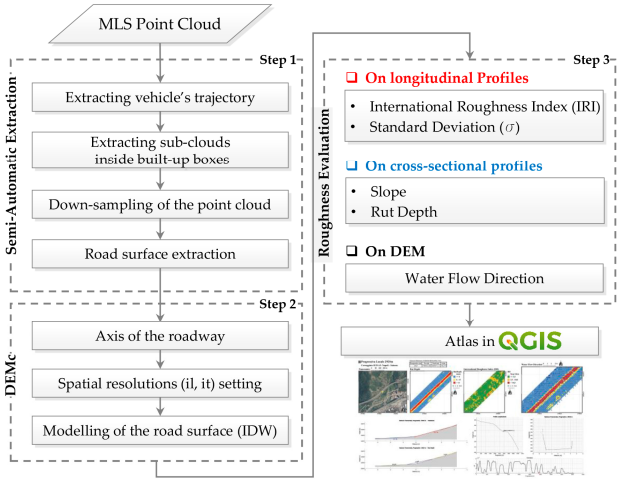

Figure 2. Data workflow

3.1 Semi-Automatic Extraction of the Road Surface

The identification of surface defects requires processing preceded by a preliminary step of filtering the raw data.

Most of the approaches and methodologies proposed in the literature to identify the edges of the road surface have been developed for some scenarios, such as the presence of great variations in height between contiguous elements at the border areas (e.g., the presence of a curb or sidewalk).

The presence of removable objects that do not belong to the road surface could be a major limitation to the success rate of these methods. There are only few extraction methods designed in situations where the edges of the road surface are not easily identifiable, mainly in rural and suburban areas.

The suggested method of extracting the road surface, based on the implementation of the methodology described in De Blasiis et al. (2020), aims to overcome the above drawbacks.

It is divided into four steps:

1. Extracting the vehicle's trajectory from the LAS data. To extract from the whole cloud of laser points only a few points that will be the vertexes of the polyline representative of the vehicle's trajectory, the points acquired with a given scanning angle are extracted. Generally, a scan angle of 0 deg is associated with the vehicle trajectory.
2. Extracting sub-clouds inside built-up boxes. To reduce the CPU time, the whole point cloud has been divided into many sub-clouds, whose points are contained into polygonal boxes purposely built to divide it. The vertices of the boxes are aligned in a direction orthogonal to the polyline that describes the trajectory of the vehicle.
3. Down-sampling of the point cloud. The step consists of down sampling the point cloud to obtain the nodes that are used as the center of the research spheres for the follow-up road surface extraction process. A regular voxel grid is built with a user assigned step (Figure 3).

Nodes whose normal vector has a component along the z axis (with z in the direction of the ellipsoidal height) of less than 1 (with a margin of error of 5×10^{-3}) have been removed.

4. Road surface extraction. In the last editing step, the M-estimator SAmple Consensus (MSAC) algorithm has been used, which is a robust variant of the Random Sample Consensus (RANSAC) algorithm, an iterative method to estimate the parameters of a mathematical model from a set of observed data that contains outliers.

The main variables of the function are: the "maxDistance" between the plane and the generic point so that it can be considered an inlier (dp, Figure 4), the "ReferenceVector" (Rv, Figure 4) which is a constraint on the orientation of the reference plane, and the "maxAngularDistance" (φ, Figure 4), which is a threshold value for the angular distance between the normal vector of the fitted plane and another vector (in the direction of the ellipsoidal height).

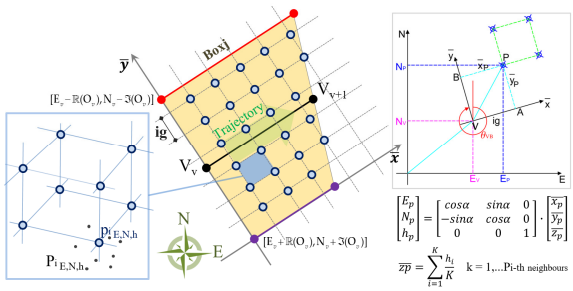

Figure 3. Voxel grid on a single box.

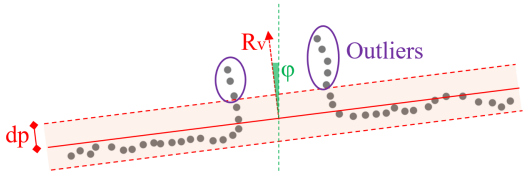

Figure 4. Parameters of MSAC algorithm.

3.2 Modelling of the road surface

The particular plano-altimetric development of the road belt makes the classic methods used for DEM extraction unsuitable, on which most modelling software is based, which reconstruct the trend of a given variable according to a regular grid of nodes starting from discrete measured and irregularly distributed values. This is done by means of interpolation techniques that allow the creation of a statistical or deterministic surface, usually in matrix format with a resolution chosen by the user; each element of the matrix corresponds to an elevation value. However, it is evident that a grid structure oriented according to the North-South cartographic grid is not effective to represent the curvilinear development of a road infrastructure.

To overcome this issue, a specific algorithm able to generate a curved abscissa grid, called DEMc, has been studied and implemented. The methodology used is detailed in Barbarella et al. (2022).

The direction of the abscissa (L, Figure 5) follows the axis of the road. The curved grid is organized in a matrix at different levels, composed by *n* rows equal to the number of nodes constituting the generic longitudinal profile and by *c* columns equal to the number of nodes constituting the generic cross section (Figure 5). The construction of this model, represented by a 'raster' matrix $D\epsilon\Re^{n,c}$, is semi-automatic.

The elevation value of each single node of the two-dimensional grid is estimated through specially modified spatial and local interpolation processes. The spatial resolutions (*il*, *it*) is chosen according to the type of distress to be analyzed, which in turn affects the acquisition rate and consequently the density of the point cloud.

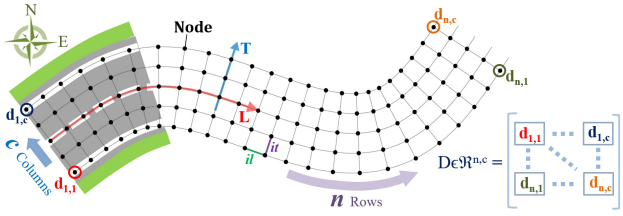

Figure 5. DEMc.

The presence of obstacles on road pavement having significant longitudinal/cross-sectional development or the presence of vehicles result in areas with missing data on the pavement. If the search radius of the chosen spatial interpolator around the generic node is smaller than the size of the shadow zone, no elevation value will be associated with the node. To overcome this problem, a search radius equal to the dimensions of the shaded area could be set; this, however, would produce over-smoothing of the whole pavement model. To avoid the pointed-out issues, the interpolation of the elevation values of each individual node of the curved grid is based on two steps:
The first step is iterative, with variable radius (r, Figure 6) of the search sphere with barycenter in the generic node; fixed the initial value of the radius, it will be increased until it reaches the preset maximum value, until the number of points contained within it is equal to the minimum number preset. If the assigned minimum number of points is not contained within the Maximum radius search sphere, a *NaN* will be associated with the node elevation. The minimum and maximum value of the search radius will be a function of the DEM resolution. Given that the use of exact interpolators does not result in significant variation in elevation values (De Blasiis et al., 2021), resulting in differences in values that are less than the accuracy of the technique, the value to be assigned to the node of the DEMc grid has been estimated using the Inverse Distance to a Power (IDW) algorithm.

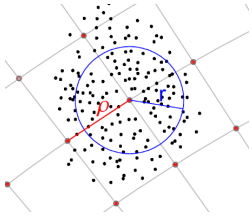

Figure 6. Search sphere around the single node (red dot), r is the variable radius of the search sphere.

The second step is based on the column-wise analysis of the D matrix containing the interpolated elevation values of the nodes. At *NaN* values the algorithm fills missing values according to the data in each column by linear interpolation. So, it is possible to rebuild the trend of the road surface avoiding underfitting or overfitting effects.

3.3 Roughness Evaluation on DEMc

Roughness Evaluation resulted from the analysis of single longitudinal (L) and cross-sectional (T) profiles, as shown in Figure 5.

3.3.1 Longitudinal Regularity. Roughness is a major parameter for the pavement surface. It depends on surface irregularities and therefore affects drive quality and road safety. The road surface roughness analysis method developed is based on the computation of two main roughness indices: The International Roughness Index (IRI) and the standard deviation of longitudinal roughness (σ) on the DEMc. In order to compute the IRI, an algorithm based on Quarter Car Simulation (QCS) (Sayers, 1995) has been implemented. The mathematics of IRI computation is:

$$IRI = \frac{1}{L}\int_0^t \left| z_s^{'} - z_u^{'} \right| dt \qquad (1)$$

where: L is the length of the road section, t is the time of the simulation, z_s' and z_u' are the vertical speeds of the sprung and unsprung mass, respectively. The main difference between the standard method (Sayers, 1995) and the method implemented is that the longitudinal sampling interval (il, Figure 5) of the profiles extracted from the curved abscissa DEMc is variable. The center profile is the only one having a constant interval il; in the curve, as one moves away from the center profile, the interval il acquires different values. This variability was, precisely, considered in the implemented algorithm.
The mathematics of σ computation is:

$$\sigma = \sqrt{\frac{n\sum d_i^2 - \left(\sum d_i\right)^2}{n(n-1)}} \qquad (2)$$

where: d_i is the deviation of the *i-th* elevation from a simple linear regression for an assigned base-length and n is the number of elevation values in the base-length (3m) (Farias et al., 2009). Both indices have been computed on each profile extracted from the DEMc of the road surface. The values are useful to identify any possible localized irregularities, such as joints and sudden jumps in elevation.

3.3.2 Cross slope. The variation of cross slope implies a rotation of the roadway or part of it around an axis, which generally does not coincide with the central axis materialized by the road signs.
The algorithm we implemented allows identifying the section type, whether double-pitch or single-pitch, and consequently estimating the centre of rotation, where the slope change occurs, this via the implementation of a process based on the RANSAC algorithm. The process is run on each individual cross-sectional profile and is based on the following steps, in the generic double-pitch case (Figure 7):
a. Linear interpolation with RANSAC algorithm of the nodes belonging to the single lane (Figure 7a);
b. Idem on the nodes of the other lane (Figure 7b);
c. Calculation of the point of intersection between the interpolated straight lines and calculation of the slopes q_1 and q_2 (Figure 7c).
Otherwise, if the following conditions are met, the entire cross-sectional profile will be treated as being a single pitch:
1. The q_1 section identified in step a. or the q_2 section identified in step b. has a length of less than 50 cm.
2. The slopes of sections q_1 and q_2 differ by an amount smaller than 0.5%.
3. There is no intersection between the two lines (q_1 and q_2) (case of parallel lines) or the point of intersection is outside the cross section.
The slopes of the single pitch or segments of the double pitch are then calculated, depending on the type of section identified.

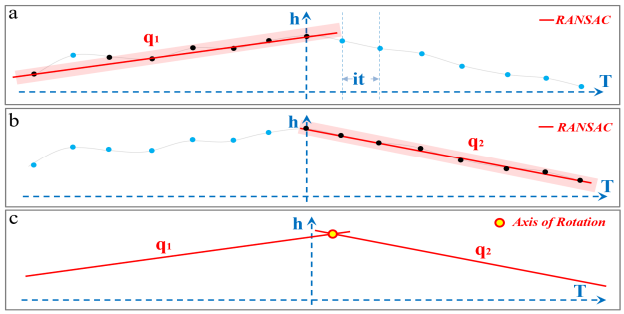

Figure 7. Identification of constant slope sections on the generic cross-sectional profile T; (a) Fit Line RANSAC first lane; (b) Fit Line second lane; (c) Center of rotation.

3.3.3 Rut depth. They have a particular configuration to collect rainwater thus promoting aquaplaning phenomena.
The implemented algorithm is based on the "Straight-Edge Rut Depth Algorithm" of the Strategic Highway Research Program (SHRP) of Hadley and Myers modified to fit the created digital model (Hadley et al., 1991). The algorithm allows to associate each calculated depth value with its homologous node belonging to the DEMc. In this way, the spatial trend and configuration of the deformation condition can be reconstructed. Figure 8 shows the diagram of the process that was implemented to simulate the straight edge lying on the generic cross-sectional profile. The main parameters to be set are two: the minimum (L_{MIN}) and maximum (L_{MAX}) length of the Straight-Edge.

Starting from the first node $P_{START}(L_{i=1},h_{i=1})$, with i = 1, the direction angle $\vartheta_{START,i}$, and the distance d_i for each section between P_{START} and the generic P_i node is calculated (Figure 8a). Then the P_i node having an elevation h_i that results in a smaller direction angle $\vartheta_{START,i}$ is selected; this is called $P_{STOP}(L_i,h_i)$ (Figure 8a). If the distance between P_{START} and P_{STOP} is smaller than the minimum set length (L_{MIN}), the cycle repeats starting from the last identified node $P_{STOP}(L_i,h_i)$ (Figure 8b). Whereas, if the distance between P_{START} and P_{STOP} is between the two set distances [L_{MIN} - L_{MAX}], a line *r* passing through the two nodes is constructed so as to simulate the Straight-Edge (Figure 8c).
That is, the generic Straight-edge will have to have a distance within the range [L_{MIN} - L_{MAX}] and a minimum direction angle ϑ. The algorithm analyzes all DEMc cross profiles, i.e., all rows of the D matrix, and will associate each DEMc node with the calculated rut depth value (Figure 8c), so as to obtain the spatial pattern of the rut.

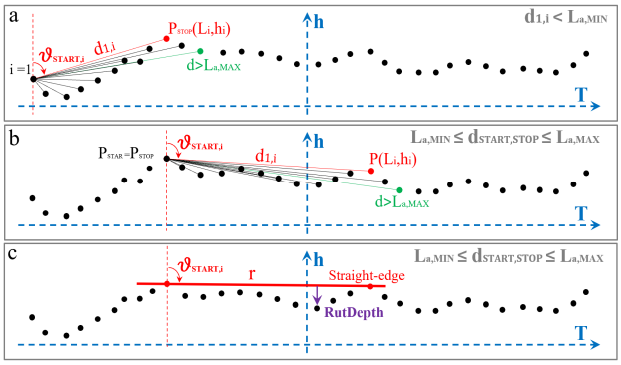

Figure 8. Example application of the Straight-Edge Rut Depth Algorithm on the generic cross-sectional profile T; (a) Iterative cycle with conditions not satisfied; (b) Iterative cycle with conditions satisfied; (c) Rule generation and calculation of ruth depths on each node.

3.3.4 Water Flow Direction. The implemented process also allows the determination of rainwater flow directions, which, together with the rut depth analysis, makes it possible to analyse possible water flows and accumulations that mainly affect the safety of users during rainfall or post-rain events. Water accumulations at rutting can cause aquaplaning phenomena, so estimation of water flows, mainly on highways, is a key issue for users' safety. Water flow direction is calculated using the D8 algorithm introduced by O'Callaghan and Mark (1984) on the DEMc of pavement. This model is one of the most widely used in hydrology since it appears to have a strong positive correlation between the observed water flow over the test area and that modeled with the proposed algorithm. The result confirms the effectiveness of the D8 model in providing a fast assessment of the potential water flow variability.

4. RESULTS

4.1 Semi-Automatic Extraction of Road Surface

The polygonal boxes were built around the trajectory of the vehicle reconstructed by extracting from the MLS point cloud the only points with a scanning angle of 0 degree (with a margin of error of 5×10^{-3}). These points were interpolated linearly to construct a polyline made of 5 m long sections. On the points belonging to each box, a voxel grid (step size 0.20 m) has been built to down-sample the original point cloud. On the nodes of the voxel grid the MSAC-based plane fitting algorithm was run, and a sphere with a diameter 3 times the grid step, namely 0.60 m, has been built to remove the outliers.
In the tests a threshold absolute value "maxDistance" (dp) of 2.5 cm, within the range of values corresponding to the pavement's macro-texture, was set. The "maxAngularDistance" (φ) value being used is 10°, since larger values do not produce effective filtering (De Blasiis et al., 2020).

4.2 Modelling of the road surface

The DEMc of the road pavement was created as described in Section 3.2 starting from the points classified as ground. The curved abscissa DEMc is generated starting from the axis polyline of the roadway. The axis polyline is extracted by analyzing the intensity values of the horizontal markings of the roadway axis, then this is interpolated with a B-spline in order to reconstruct the curvilinear trend. A resolution (it and il) of 10 cm was chosen, both longitudinally and crosswise since the analysis aims at determining surface deformations and calculating localized IRI (Barbarella et al. 2022).
The nodes of the curved grid were interpolated using the local interpolator IDW^2, the minimum search radius was set equal to 7 cm, the maximum radius equal to 3 times the minimum. The minimum number of points for interpolation was set equal to 50.
A total of 45,938 cross-sectional profiles, one every 10 cm, and 65 longitudinal profiles, one every 10 cm, were analyzed for a road width of 6.40 m and a section length of 4,593.70 m.
Figure 9a shows a perspective view of the nodes of the DEMc of the pavement (white dots) and two perspective views of the overlay of the nodes to the original point cloud (Figure 9b,c). Please note how the algorithm filtered out the vehicles present on the acceleration lane (the surveyed section was open to traffic) and the vertical marking present. This made it possible to reconstruct the pavement surface even at shaded areas due to the presence of obstacles, vertical marking, and vehicles.

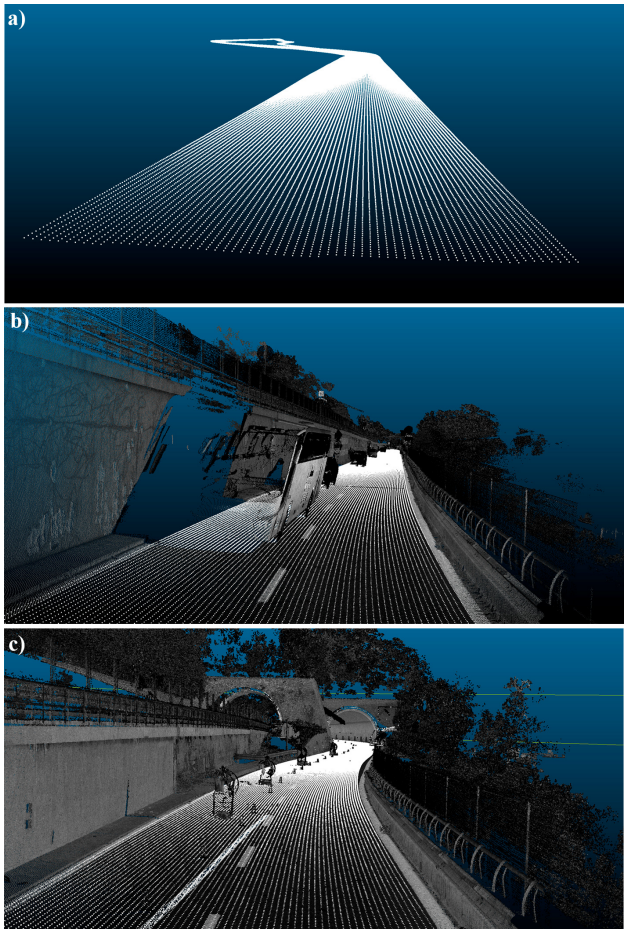

Figure 9. (a) Perspective view of the DEMc nodes; (b, c) Perspective view of the DEMc nodes overlaid on the input point cloud.

4.3 Roughness Evaluation and Atlas building

Longitudinal regularity was analyzed on each longitudinal profile of the DEMc. At each grid node, the IRI index and standard deviation of the differences in elevation values from a 3 m baseline were calculated.

A total of 65 longitudinal profiles 4,593.70 m long were analyzed, each at 10 cm spacing: the central axis of the roadway, 32 profiles to the right and 32 to the left of the axis, the direction is concordant with the driving direction of the section, i.e., from km 46+800 to km 51+600.

The punctual values of the regularity indicators highlight any localized defects compared to the values averaged over the standard length from the regulation. The punctual values are associated with each individual node of the DEMc, and this can be imported into a GIS environment as a punctual shapefile. The attribute table will contain the IRI or σ values of each node. Next, classified maps were generated according to standards (Figure 10 a3-b3). On the atlas, only the map with IRI values was shown since the σ values appear to be correlated (Farias et al., 2009).

Cross-sectional regularity (slope and rut depth) is calculated on each cross-sectional profile. A total of 45,938 cross-sectional profiles were analyzed, corresponding to the rows of the D matrix of the DEMc.

As with the IRI index, the point values of rut depths are associated with each individual node of the DEMc so as to import the shapefile into GIS and produce a classified map of the rutting according to the levels of severity listed in the regulations (Figure 10 a2-b2). All results are produced in order to build an atlas in QGIS environment in a semiautomatic way. All tables and cross-sectional profiles are saved in .svg with a name so as to do automatic hyperlinking.

Figure 10 shows an example of two atlas tables. The atlas is structured to have a general overview of the single cross-sectional profile analyzed (Figure 10 a-b).

Panels a2-b2 show the rut depth maps, the red line marks the planimetric position of the generic profile analyzed and visible in panels a5-b5, a6-b6, a9-b9. Panels a3-b3 show the graded IRI map in order to highlight the strong variations, which are a symptom of localized irregularities due, for example, to the presence of potholes, joints, or bumps. Panels a4-b4 show the water flow direction vectors superimposed on the rut depth maps. Panels a5-b5 show the cross section with estimated cross-sectional contour and determination of slope and center of rotation. Panels a6-b6 show the cross-section of the analyzed progressive with straight-edge simulation and maximum rut depth values. Panels a7-b7 show the longitudinal profile, the red cross marks the location of the cross profile shown in panels a5-b5, a6-b6, a9-b9. Panels a8-b8 show the graph of experimental curvature (1/R) for estimating the planimetric direction of the DEM axis: local maximums (1/R = max) identify sections in curve with constant radius; null values (1/R = 0) identify sections in straight; finally, intermediate values (0<1/R<max) identify sections with variable curvature, clothoid. Lastly, panels a9-b9 show the cross sections of the input point cloud having a thickness of 5 cm.

Panels (a) and (b) in Figure 10 report two atlas tables for two different road section configurations.

Panel (a) reports the analysis of the local 2,940 m progressive and shows a case where the water flow tends to accumulate in the centerline due to the counter-slope of the section and the rutting having high severity level present on the whole portion of the pavement analyzed. Comparing the IRI map (panel a3) and the rut depth map (panel a2), it is possible to observe that localized irregularity is present both crosswise and longitudinal. Combining the two pieces of information is important; a rut produced by the passage of vehicles has a fairly regular longitudinal and crosswise development located, generally, at the vehicle wheel trace. A strong localized rutting with a small longitudinal development, such as a depression or pothole, will produce an abrupt vertical acceleration in the quarter Car model and this will correspond to a strong local variation in IRI values (isolated red area, panel a3). Longitudinal profile analysis shows that the section is located at a "downslope" section (panel a7), and, of course, the water flow goes from southwest to northeast, channeling at the strong rutting (panel a4). The analysis of the planimetric trend shows that the subject section is in the transition zone between straight and the beginning of clothoid (panel a8).

Panel (b) in Figure 10 shows a section located in tunnel at the local progressive 4,320 m (panel b9) and rectilinear (panel b8). Analyzing the IRI map, the longitudinal trend is quite regular, no particular localized effects are shown (panel b3). The cross section is very regular, the rut depth values fall within the low severity level (panels b2, b6). The cross-section is double pitch with slopes such that water flows away from the centerline toward the roadsides (panel b4) but still the slopes are below the standard threshold set at 2.5%.

5. CONCLUSIONS

In present work, attention has been paid to highlight the potential of using the LiDAR survey technique, one of the most interesting and continuously developing remote sensing techniques, to assess the "state of degradation" of the road pavement. The technique has proved to be effective in providing data that allow us to build a 3D model of the infrastructure surface. Given that the applications of the technique to infrastructure surveying are recent, there are still many critical issues to address. Commercial software available implement only a few functions, in response to the specific needs of professionals and, therefore, do not fully satisfy the scientific community. To overcome these limitations, several issues that arise in the application of the technique to road survey have been analysed and some algorithms have been implemented in proprietary software (in MATLAB environment) and tested on a few case studies.

The results obtained with the proposed methods depend mainly on the value of the parameters given as input to the implemented algorithms. In the editing phase, it is important to choose the correct values because the reconstructed 3D model of the road surface represents the reference surface on which the distresses will be highlighted.

The choice of some parameters is based on considerations related to the nature of the input data: the DEMc resolution, for example, is in relation to the characteristics of the point cloud, i.e., its density and accuracy. Other parameters have been chosen according to the roughness indices to be computed or to the type of distress to be identified. For others, some tests have been carried out to verify the influence of the choice of certain values on the results.

The sudden deterioration in the condition of the infrastructure network has made road preservation and management a complex task. The problem is further compounded by the limited resources available for monitoring, maintenance, and rehabilitation operations. In most cases, due to limited funds and personnel, the traditional data acquisition process is very slow and expensive.

The MLS surveys were done one-way and at night, avoiding the interruption of traffic, to assess the potential while minimizing interference and acquisition times.

The implemented process made it possible to draw up an atlas in a GIS environment in a few working hours in a semi-automatic way, which is useful to the managing authority for the identification of the sections where it is necessary to draft a program of first intervention.

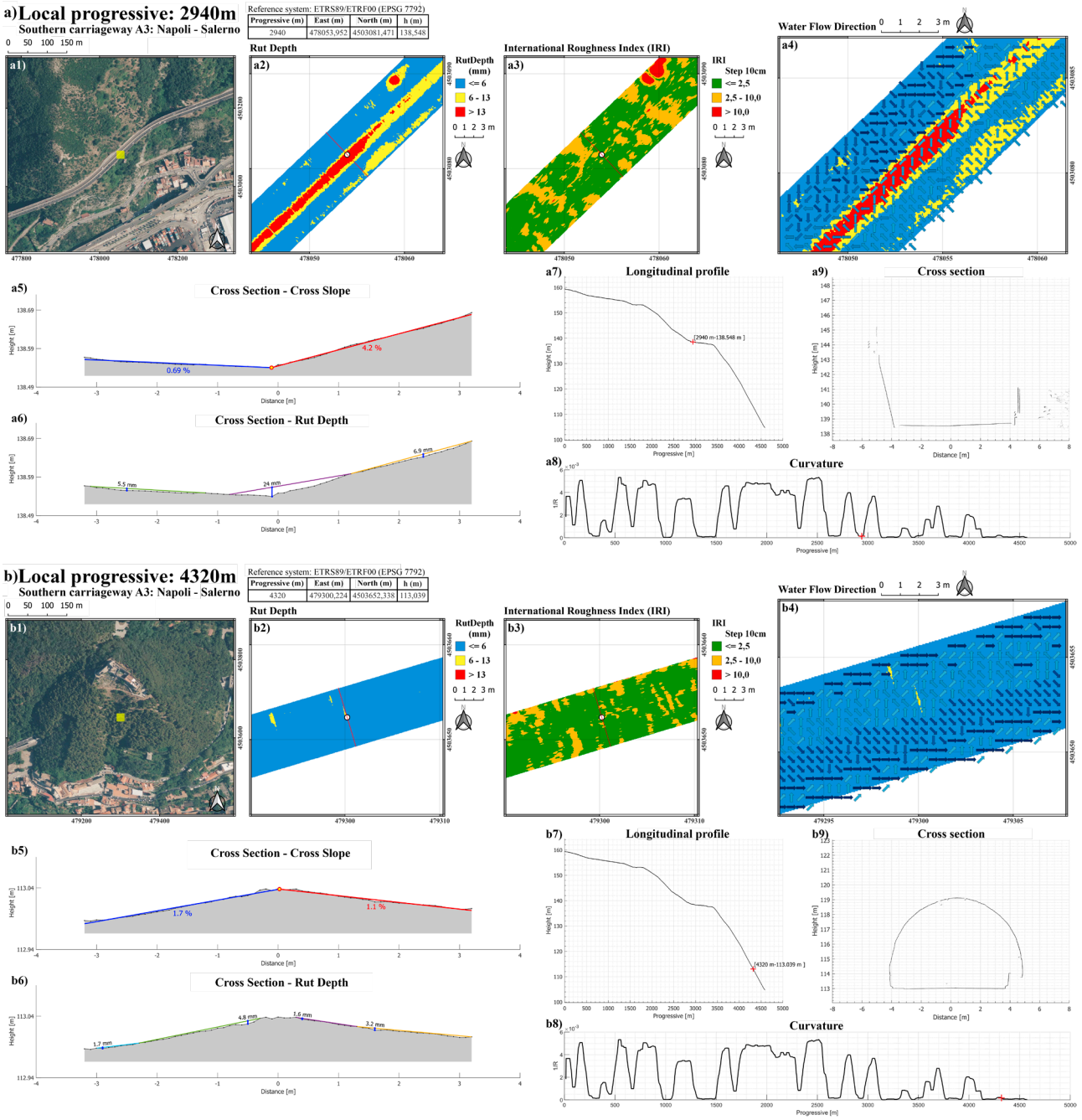

Figure 10. Atlas in QGIS. (a) Local progressive 2,940 m; (b) Local progressive 4,320 m; (a1-b1) Panoramic overview, yellow square marks the stretch of road analyzed (Google Maps); (a2-b2) and (a3-b3) Rut Depth and IRI map, red line marks the analyzed profile; (a4-b4) Water Flow Direction vectors overlaid on the Rut Depth map; (a5-b5) Cross-section with Slope analysis; (a6-b6) Cross-section with Straight-edge simulation with the maximum rut depth values; (a7-b7) Longitudinal Profile, the red cross pinpoints the location of the cross-sectional profile; (a8-b8) Experimental curvature diagram, the red cross pinpoints the location of the cross-sectional profile; (a9-b9) Cross-sectional point cloud.

ACKNOWLEDGEMENTS

We would like to thank C.U.G.RI. (Inter-University Research Center for the Prediction and Prevention of Major Hazards), Leica Geosystems for the collaboration in field survey operations and the Consorzio Stabile SIS S.c.p.a. for the logistical support and assistance.

REFERENCES

Alhasan, A., White, D.J., De Brabanter, K., 2017. Spatial pavement roughness from stationary laser scanning. *International Journal of Pavement Engineering* 18, 83-96.

ASTM, D6433-18, 2018. Standard Practice for Roads and Parking Lots Pavement Condition Index Surveys. ASTM International, West Conshohocken, PA.

Balado, J., Díaz-Vilariño, L., Arias, P., González-Jorge, H., 2018. Automatic classification of urban ground elements from mobile laser scanning data. *Automation in Construction* 86, 226-239.

Barbarella, M., Di Benedetto, A., Fiani, M., 2022. A Method for Obtaining a DEM with Curved Abscissa from MLS Data for Linear Infrastructure Survey Design. *Remote Sens.* 14, 889.

Barbarella, M., D'Amico, F., De Blasiis, M., Di Benedetto, A., Fiani, M., 2018. Use of Terrestrial Laser Scanner for Rigid Airport Pavement Management. *Sensors* 18, 44.

Barbarella, M., De Blasiis, M.R., Fiani, M., 2017. Terrestrial laser scanner for the analysis of airport pavement geometry. *International Journal of Pavement Engineering*, 1-15.

Barber, D., Mills, J., Smith-Voysey, S., 2008. Geometric validation of a ground-based mobile laser scanning system. *ISPRS Journal of Photogrammetry and Remote Sensing* 63, 128-141.

Chang, J., Chang, K., Chen, D., 2006. Application of 3D Laser Scanning on Measuring Pavement Roughness. *Materials Science*.

Che, E., Jung, J., Olsen, M.J., 2019. Object Recognition, Segmentation, and Classification of Mobile Laser Scanning Point Clouds: A State of the Art Review. *Sensors* 19, 810.

Chin, A., 2012. Paving the way for terrestrial laser scanning assessment of road quality. MSc dissertation. Oregon State University, USA.

De Blasiis, M.R., Di Benedetto, A., Fiani, M., Garozzo, M., 2021. Assessing of the Road Pavement Roughness by Means of LiDAR Technology. *Coatings* 11, 17.

De Blasiis, M., Di Benedetto, A., Fiani, M., Garozzo, M., 2019a. Characterization of road surface by means of laser scanner technologies, Pavement and Asset Management: *Proceedings of the World Conference on Pavement and Asset Management (WCPAM 2017)*, June 12-16, 2017, Baveno, Italy. CRC Press, p. 63.

De Blasiis, M.R., Di Benedetto, A., Fiani, M., 2020. Mobile Laser Scanning Data for the Evaluation of Pavement Surface Distress. *Remote Sensing* 12, 942.

De Blasiis, M.R., Di Benedetto, A., Fiani, M., Garozzo, M., 2019b. Assessing the Effect of Pavement Distresses by Means of LiDAR Technology, *ASCE International Conference on Computing in Civil Engineering 2019 American Society of Civil Engineers*.

Díaz-Vilariño, L., González-Jorge, H., Bueno, M., Arias, P., Puente, I., 2016. Automatic classification of urban pavements using mobile LiDAR data and roughness descriptors. *Construction and Building Materials* 102, 208-215.

Farias, M., O. de Souza, R., T Harvey, J., A Bukhari, S., 2009. Correlations and Analyses of Longitudinal Roughness Indices. *Road Materials and Pavement Design* 10(2), 399-415.

Fryskowska, A., Wróblewski, P., 2018. Mobile Laser Scanning accuracy assessment for the purpose of base-map updating. *Geodesy and Cartography* 67, 35-55.

Gandolfi, S., Barbarella, M., Ronci, E., Burchi, A., 2008. Close photogrammetry and laser scanning using a mobile mapping system for the high detailed survey of a high density urban area. *International Archives of the Photogrammetry, Remote Sensing and Spatial Information Sciences* 37, 909-914.

Glennie, C., 2007. Rigorous 3D error analysis of kinematic scanning LIDAR systems, *Journal of Applied Geodesy*. 147.

Glennie, C., 2009. Kinematic terrestrial light-detection and ranging system for scanning. *Transportation Research Record: Journal of the Transportation Research Board*, 135-141.

Guan, H., Li, J., Cao, S., Yu, Y., 2016. Use of mobile LiDAR in road information inventory: a review. *International Journal of Image and Data Fusion* 7, 219-242.

Guan, H., Li, J., Yu, Y., Wang, C., Chapman, M., Yang, B., 2014. Using mobile laser scanning data for automated extraction of road markings. *ISPRS Journal of Photogrammetry and Remote Sensing* 87, 93-107.

Hadley, W.O. and Myers, M.G., 1991. Rut Depth Estimates Developed from Cross Profile Data. AU-179. *Texas Research and Development Foundation*, Austin.

Harvey, J., Meijer, J., Kendall, A., 2014. Life Cycle Assessment of Pavements:[techbrief]. United States. *Federal Highway Administration*.

Ibrahim, S., Lichti, D., 2012. CURB-BASED STREET FLOOR EXTRACTION FROM MOBILE TERRESTRIAL LIDAR POINT CLOUD. *Int. Arch. Photogramm. Remote Sens. Spatial Inf. Sci.* XXXIX-B5, 193-198.

Zeybek, M. and Serkan B., 2023. Road surface and inventory extraction from mobile LiDAR point cloud using iterative piecewise linear model. *Measurement Science and Technology*, 34(5), 055204.

Křemen, T., Štroner, M., Třasák, P., 2014. Determination of Pavement Elevations by the 3D Scanning System and Its Verification. *Geoinformatics FCE CTU* 12, 55-60.

Kumar, P., Angelats, E., 2017. AN AUTOMATED ROAD ROUGHNESS DETECTION FROM MOBILE LASER SCANNING DATA. *Int. Arch. Photogramm. Remote Sens. Spatial Inf. Sci.* XLII-1/W1, 91-96.

Kumar, P., Lewis, P., Mc Elhinney, C., Rahman, A., 2015. An Algorithm for Automated Estimation of Road Roughness from Mobile Laser Scanning Data. *Photogramm. Rec*. 30, 30–45.

Kumar, P., McElhinney, C.P., Lewis, P., McCarthy, T., 2013. An automated algorithm for extracting road edges from terrestrial mobile LiDAR data. *ISPRS Journal of Photogrammetry and Remote Sensing* 85, 44-55.

Kumar, P., McElhinney, C.P., Lewis, P., McCarthy, T., 2014. Automated road markings extraction from mobile laser scanning data. *International Journal of Applied Earth Observation and Geoinformation* 32, 125-137.

Liu, C., Liu, Y., Chen, Y., Zhao, C., Qiu, J., Wu, D., ... & Tang, K., 2023. A state-of-the-practice review of three-dimensional laser scanning technology for tunnel distress monitoring. *Journal of Performance of Constructed Facilities* 37(2), 03123001.

Mc Elhinney, C., Kumar, P., Cahalane, C., McCarthy, T., 2010. Initial results from European Road Safety Inspection (EURSI) mobile mapping project. *Proceedings of ISPRS CRIMT, Newcastle.*

O'Callaghan, J. F., and Mark, D. M., 1984. The extraction of drainage networks from digital elevation data. *Computer Vision, Graphics and Image Processing* 28, 323-344.

Ragnoli, A., De Blasiis, M.R., Di Benedetto, A., 2018. Pavement Distress Detection Methods: A Review. *Infrastructures* 3, 58.

Romero, L.M., Guerrero, J.A., Romero, G., 2021. Road Curb Detection: A Historical Survey. *Sensors* 21, 6952.

Salini, R., Xu, B., Paplauskas, P., 2017. Pavement Distress Detection with PICUCHA Methodology for Area-Scan Cameras and Dark Images. *Stavební Obzor-The Civil Engineering Journal* (1), 34-45.

Sayers, M.W., 1995. On the calculation of international roughness index from longitudinal road profile. *Transportation Research Record*.

Shen, G., 2016. Road crack detection based on video image processing, 2016 *3rd International Conference on Systems and Informatics (ICSAI)*, 912-917.

Toschi, I., Rodríguez-Gonzálvez, P., Remondino, F., Minto, S., Orlandini, S., Fuller, A., 2015. ACCURACY EVALUATION OF A MOBILE MAPPING SYSTEM WITH ADVANCED STATISTICAL METHODS. *Int. Arch. Photogramm. Remote Sens. Spatial Inf. Sci.* XL-5/W4, 245-253.

van der Horst, B.B., Lindenbergh, R.C., Puister, S.W.J., 2019. MOBILE LASER SCAN DATA FOR ROAD SURFACE DAMAGE DETECTION. *Int. Arch. Photogramm. Remote Sens. Spatial Inf. Sci*. XLII-2/W13, 1141-1148.

Yadav, M., Singh, A.K., Lohani, B., 2017. Extraction of road surface from mobile LiDAR data of complex road environment. *International Journal of Remote Sensing* 38, 4655-4682.

Yang, B., Fang, L., Li, J., 2013. Semi-automated extraction and delineation of 3D roads of street scene from mobile laser scanning point clouds. I*SPRS Journal of Photogrammetry and Remote Sensing* 79, 80-93.

Yen, K.S., Ravani, B., Lasky, T.A., 2011. LiDAR for data efficiency. Washington (State). Dept. of Transportation. Office of Research and Library Services.

Yoon, J., Crane, C.D., 2009. Evaluation of terrain using LADAR data in urban environment for autonomous vehicles and its application in the DARPA urban challenge, 2009 ICCAS-SICE, pp. 641-646.